Designing a Physically Realizable Electromagnetic Cloak

Heidi Slater

Advisor: Steven Cummer

Submitted for Graduation with Departmental Distinction
in Electrical and Computer Engineering

November 28, 2011

1 Abstract

Electromagnetic cloaking has been shown to successfully shield objects within the cloak from electromagnetic waves using ideal material parameters. These ideal parameters for permittivity and permeability present an issue when attempting to design a broadband cloak in which the velocity of waves within the cloak do not exceed the speed of light. This is addressed by embedding the entire cloak structure in a background dielectric with index of refraction greater than 1, such that the desired parameters are increased by the same scale factor. This paper describes the design of a cloak with parameters which are physically realizable while still maintaining performance comparable to the ideal case.

2 Introduction

Transformation optics allows for the design of materials which can bend light in a particular desired manner [1, 2]. This can be achieved using a coordinate transform, essentially transforming the original space to a set of coordinates such that an electromagnetic wave exists only within those coordinates. Because Maxwell's equations do not vary when coordinates are transformed, equations for permittivity and permeability can be obtained for the transformed coordinates. From these equations one can design an anisotropic material with specific desired characteristics. One application of this is in the design of an invisibility cloak, such that any object within the cloak will not interact with electromagnetic waves at all. One such design, as described by Cummer et al. [3], is a concentric cylindrical shell.

A simplification of this is to consider the 2D case, where the cylindrical shell is reduced to a circular shell. The coordinate transform which describes the cloak, then, is essentially taking a circular area and squeezing it into a shell with the same outer radius such that anything within that shell will not interact with electromagnetic waves. This coordinate transformation is given in [3], with the equations for the desired material properties reproduced here. A cloaking shell with inner radius R_1 and outer radius R_2 would have the following permittivity and permeability:

$$\epsilon_r = \mu_r = \frac{r - R_1}{r}, \quad \epsilon_\phi = \mu_\phi = \frac{r}{r - R_1}, \quad \epsilon_z = \mu_z = \left(\frac{R_2}{R_2 - R_1}\right)^2 \frac{r - R_1}{r} \tag{1}$$

However, these constraints can be simplified if we assume a transverse-electric (TE) wave. In this case, the only nonzero components of the electric and magnetic fields are E_z, H_r, H_ϕ. Thus, the only parameters which are important to the functionality of the cloak are ϵ_z, μ_r, and μ_ϕ. Equation 1 simplifes to:

$$\mu_r = \frac{r - R_1}{r}, \quad \mu_\phi = \frac{r}{r - R_1}, \quad \epsilon_z = \left(\frac{R_2}{R_2 - R_1}\right)^2 \frac{r - R_1}{r} \tag{2}$$

This cloak, however, requires μ and ϵ values which go to 0 on the inner radius of the cloak. The problem with this is that the group velocity of a wave cant exceed the speed of light in free space. The group velocity is the speed at which energy is transmitted in the wave, and thus must adhere to the following constraint [4, 5]:

$$v_g = \frac{d\omega}{dk} = \frac{c}{n + \omega \frac{dn}{d\omega}} = \frac{c}{\sqrt{\mu\epsilon} + \omega \frac{d\sqrt{\mu\epsilon}}{d\omega}} < c \tag{3}$$

The second term of the denominator is clearly frequency-dependent, so in order to design a broadband cloak which works over a wide range of frequencies, constraints must be placed on the first term, $\sqrt{\mu\epsilon}$. This ensures that Equation 2 will be satisfied regardless of the frequency of a wave. Thus, for a TE wave, we must maintain the constraints:

$$\mu_r \epsilon_z > 1, \quad \mu_\phi \epsilon_z > 1 \tag{4}$$

Placing this restriction would greatly decrease the effectiveness of the cloak, as any value less than 1 would be abruptly cut off at 1. If we assume a cloak with $R1 = 0.1$ m and $R2 = 0.2$ m, μ_ϕ is unaffected by this lower limit because it ranges from 2 on the outer edge of the cloak to infinity on the inner edge. ϵ_z and μ_r, however, are significantly impacted by this cutoff. The cloak parameters are plotted in Figure 1, in the range from $r = R1$ to $r = R2$. As shown in Figure 1a, for $0.1 < r < 0.13$, the ϵ_z values are cut off at 1. For μ_ϕ, which originally ranges from 0.5 down to 0, all the values are cut off to 1 (Figure 1b).

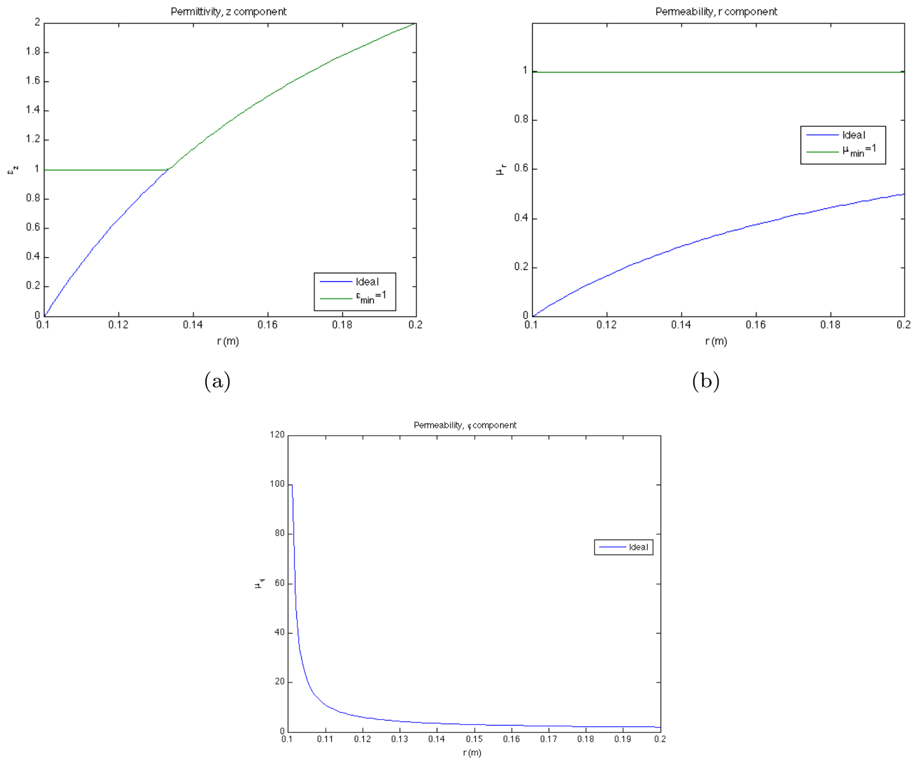

(a) (b)

(c)

Figure 1: Comparison of Cloak Parameters

One solution to this is to embed the cloak in a background material with index of refraction $n = \sqrt{\mu_r \epsilon_r} > 1$, where μ_r and ϵ_r denote relative permittivity and permeability. This approach has been used by Liu et al. in the design of a ground-plane broadband cloak [6]. For simplicity, we will assume that we are scaling μ and ϵ by the same factor, so that both are scaled by n. With an increased n, setting a minimum value of 1 will have less impact on the effectiveness of the cloak. The reasoning behind this is that the desired material parameters of the cloak from Equation 1 will all be scaled by n, so fewer values will be cut off by the minimum limit of 1. For example, if a point in the cloak had a value of $\epsilon_z = 0.4$ in air, to match a medium with $n = 3$ this value would now be scaled to $\epsilon_z = 1.2$ and would not be cut off by the $\epsilon_{min} = 1$ constraint. This concept is shown in Figure 2. ϵ_z and μ_ϕ for a cloak with $n = 3$ are plotted, and show a significant improvement over the $n = 1$ case. For ϵ_z, the cutoff point occurs at about $r = 0.11$ compared to 0.13, and for μ_r the cutoff occurs at $r = 0.15$ rather than the entire range being cut off. Based on this embedding method, the design of the cloak follows.

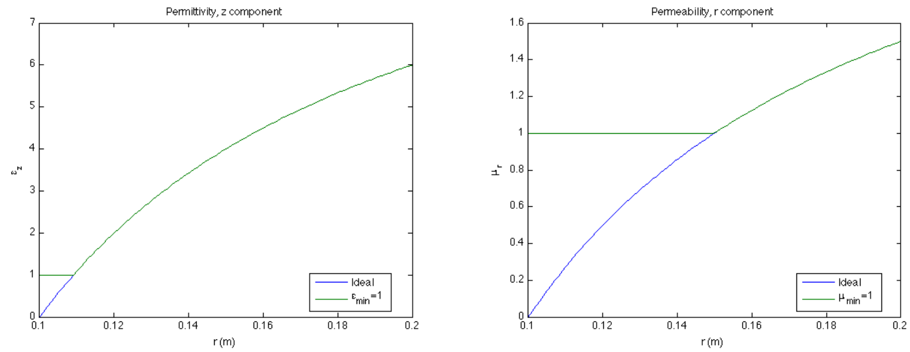

(a) (b)

Figure 2: Comparison of Cloak Parameters for $n = 3$

3 Design and Results

The cloak was designed in COMSOL Multiphysics. COMSOL allows for the simulation of arbitrary anisotropic materials, and is thus well suited for this problem. The 2D cloaking structure in [3] was used as a starting point. To simulate an unbounded region of free space, a rectangular area was surrounded by perfectly matched layers (PML) which do not cause reflection. The scattering object within the cloak in this case was a perfect magnetic conductor (PMC), and this was set as a boundary condition at the inner radius of the cloak. The design is shown in Figure 3.

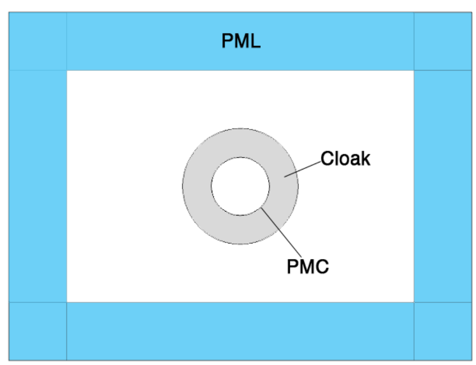

Figure 3: Simulation Design

This paper will address both transverse-electric (TE) and transverse-magnetic (TM) waves. The initial steps in the design are performed with using a TE simulation, as much of the design process is the same in both cases. A 2D simulation was performed with a TE wave at 2 GHz. This was simulated using a surface current source placed at the left boundary of the domain (at $x = -0.6$). The surface current has only a z-component, such that the electric field is only out-of-plane, and the magnetic field only in-plane. The cloak consists of a circular shell with inner radius $R1 = 0.1$ m and outer radius $R2 = 0.2$ m, with the background material being free space. The cloak has the same parameters described in Equation 2. Several simulations are shown in Figure 4. To allow for easy visual comparison of the figures, the color scales of each plot are set to the same range (-180, 180). Additionally, although the range of the data may by asymmetric, the color range is set to be symmetric. Color scales are adjusted in this same manner throughout this paper. No data is ommitted from the plot, but any data outside of the color range will appear to have the same value as the boundaries of the range. The majority of this very high field data is within the cloak, so adjusting the color range should not affect the analysis of the fields outside of the cloak.

As shown in Figure 4a, within the cloak the field is smoothly bent around the inner radius, and outside of the cloak the field is undisturbed. Without a cloak (Figure 4b), the scattering object causes reflections. Comparing Figures 4a and 4c, the field outside of the cloak in 4a is essentially indistinguishable from the case where there is no object or cloak.

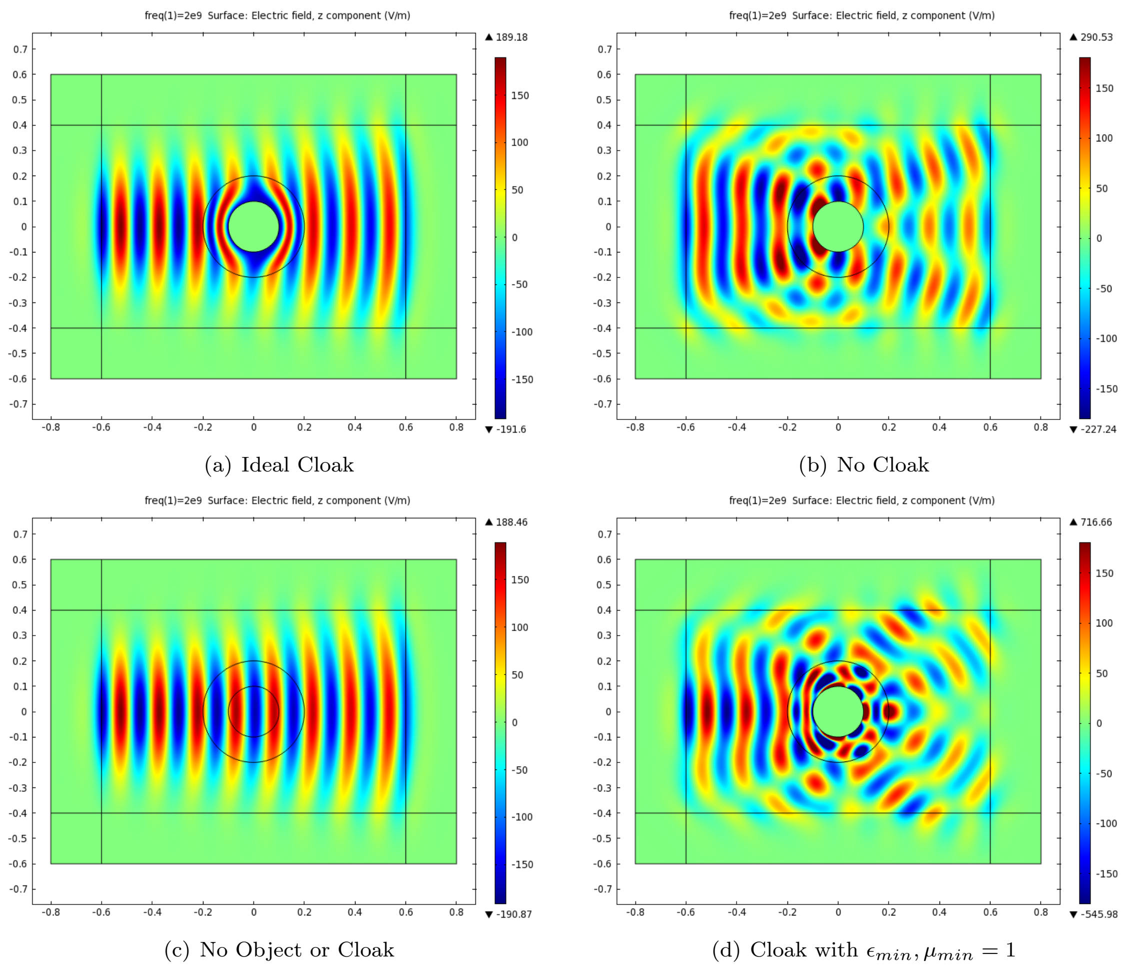

(a) Ideal Cloak

(b) No Cloak

(c) No Object or Cloak

(d) Cloak with $\epsilon_{min}, \mu_{min} = 1$

Figure 4: E_z for Cloak Simulations

However, as discussed previously, this ideal cloak requires permeability and permittivity values which go to 0. Thus, in order to design a broadband cloak the material parameters must adhere to the constraints in Equation 3. For simplicity, we begin with setting both $\epsilon_{min} = \mu_{min} = 1$. This has a significant impact on the effectiveness of the cloak, as shown in Figure 4d. In order to design the cloak within a background material with $n > 1$, a domain was created with a permittivity and permeability gradient such that the gradient begins at 1 and ends at the desired value of n. Thus, outside of this entire structure a wave should remain undisturbed. In practice a gradient ring would be more effective, but a rectangular structure was used to simplify the design and demonstrate the concept. An ideal simulation is shown for $n = 2$ in Figure 5a, with a plot of the field with no cloak given in Figure 5b for reference. Additionally, permittivity is plotted in Figure 5c to clarify the function of the gradient. (The plot for permeability is not included but would be identical.) The red arrows in Figure 5a (as well as in simulations following this) indicate time-average power flow. In performing this simulation the PML parameters are also modified such that the permittivity and permeability of the PML are equal to n everywhere. This causes a slight distortion in the gradient portion of the domain in 5a, because the PML does not perfectly match the gradient. This is a product of the simulation design and is not indicative of the effectiveness of the cloak.

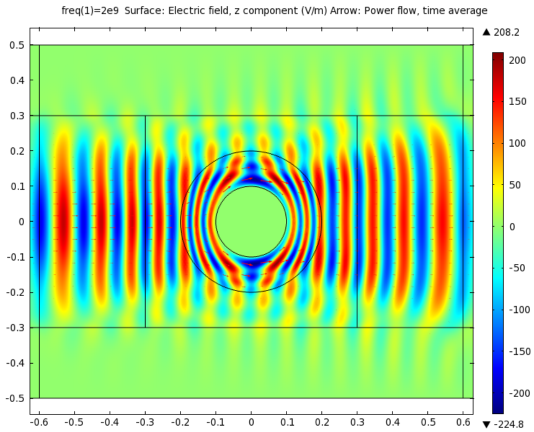

(a) Electric Field, Ideal Cloak

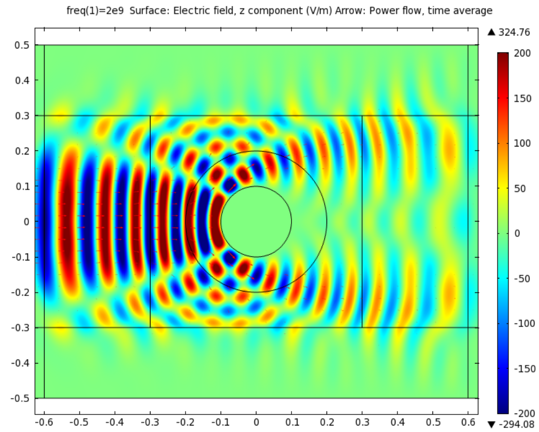

(b) Electric Field, No Cloak

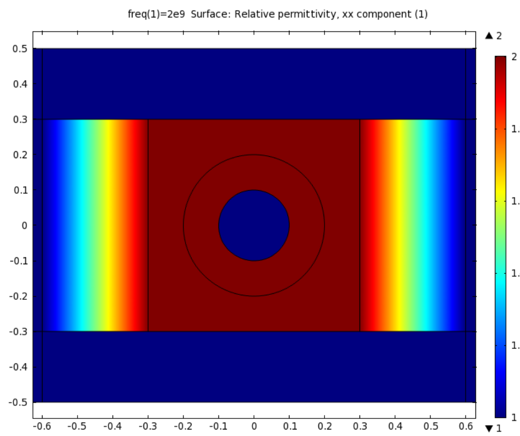

(c) Permittivity Gradient

Figure 5: Ideal Simulation for $n = 2$

Several values of n were compared to determine the benefit of increasing n, as shown in Figures 6-9. The equations which describe the cloak retain the same form as in Equation 2, but they are all scaled by n.

$$\mu_r = n\frac{r - R_1}{r}, \quad \mu_\phi = n\frac{r}{r - R_1}, \quad \epsilon_z = n\left(\frac{R_2}{R_2 - R_1}\right)^2 \frac{r - R_1}{r} \tag{5}$$

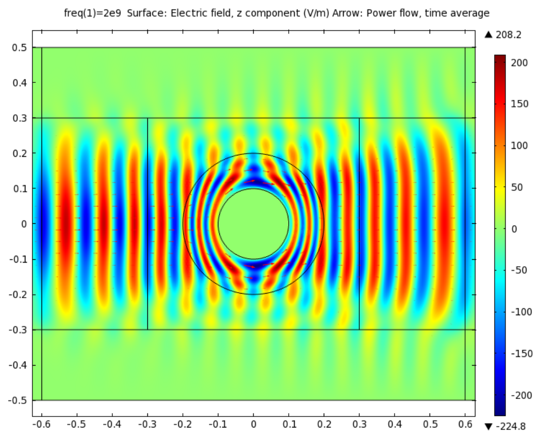

(a) Ideal Cloak

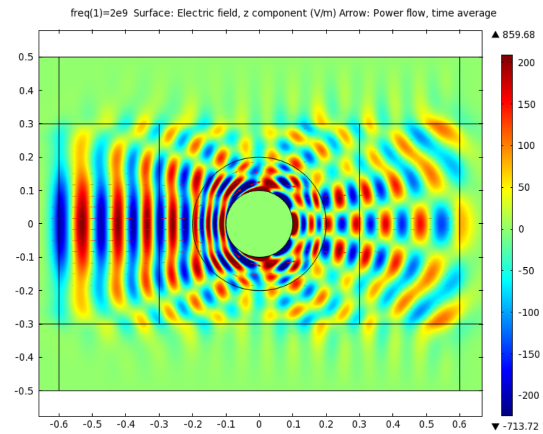

(b) Cloak with $\epsilon_{min}, \mu_{min} = 1$

Figure 6: Comparison for $n = 2$

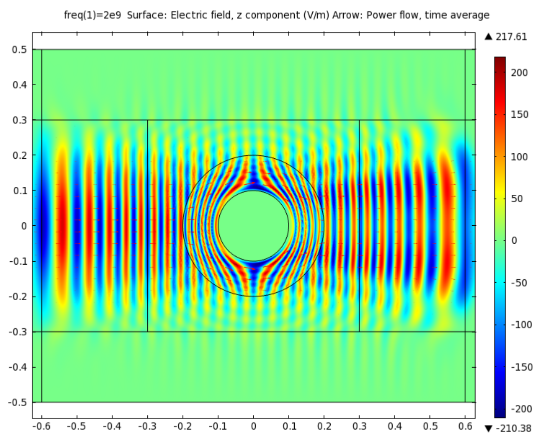

(a) Ideal Cloak

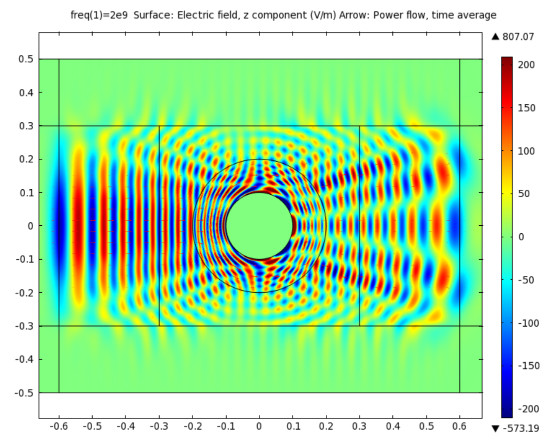

(b) Cloak with $\epsilon_{min}, \mu_{min} = 1$

Figure 7: Comparison for $n = 4$

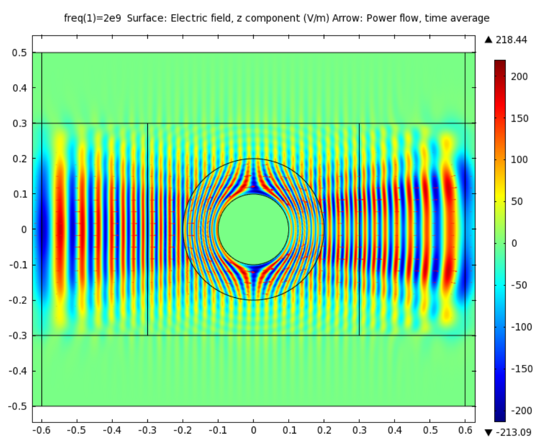

(a) Ideal Cloak

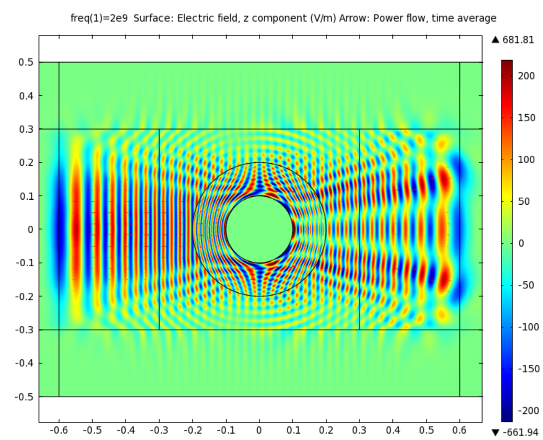

(b) Cloak with $\epsilon_{min}, \mu_{min} = 1$

Figure 8: Comparison for $n = 6$

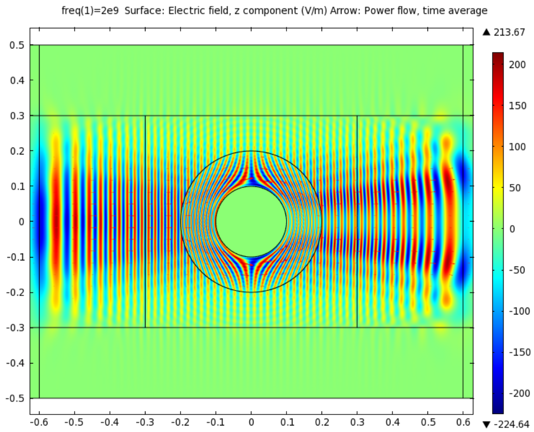

(a) Ideal Cloak

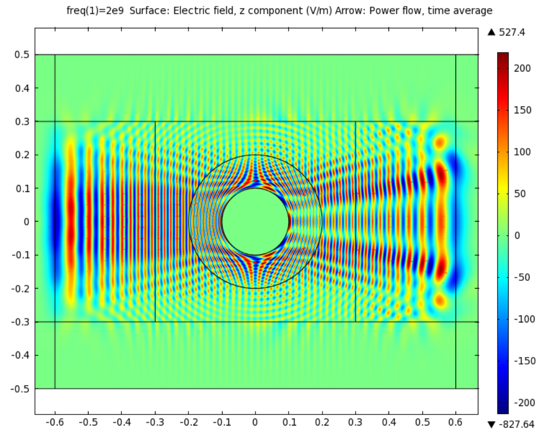

(b) Cloak with $\epsilon_{min}, \mu_{min} = 1$

Figure 9: Comparison for $n = 8$

Although an index of refraction of $n = 4$ provided a significant improvement upon $n = 2$, after this point the impact was less noticeable. Additionally, as n is increased the minimum wavelength within the material also decreases, requiring a finer mesh for the COMSOL solver and a longer computation time. To balance the tradeoff between cloak effectiveness and computation time, a background material with $n = 6$ was chosen for the remaining simulations. Referring to Figure 8, the non-ideal cloak (b) still has very good performance; although some scattering is evident it is still fairly close to the ideal case (a) and a vast improvement over the $n = 1$ case (Figure 4d). The next step was to determine which values impacted the simulation the most, and look for a pattern in the degradation of the simulation. This was done by fixing one of ϵ_{min} and μ_{min} at 0 and varying the other. The combination of these parameters is not intended to be physically realizable; the goal in this step was simply to study the effect of varying these minima. The equations which describe the cloak are specified in Equation 6.

$$\mu_r = max\left(n\left(\frac{r-R_1}{r}\right), \mu_{min}\right), \quad \mu_\phi = max\left(n\left(\frac{r}{r-R_1}\right), \mu_{min}\right),$$
$$\epsilon_z = max\left(n\left(\frac{R_2}{R_2-R_1}\right)^2, \epsilon_{min}\right) \tag{6}$$

To simplify the simulation, the gradient portion was removed, such that the background material of the entire domain has index of refraction $n = 6$. In order to measure the scattering of the electric field, points along a circle of radius $r = 0.4$ m were extracted and analyzed. This is the outermost circle shown in Figure 10. No boundary condition is placed on this circle; it was added specifically for the purpose of extracting data.

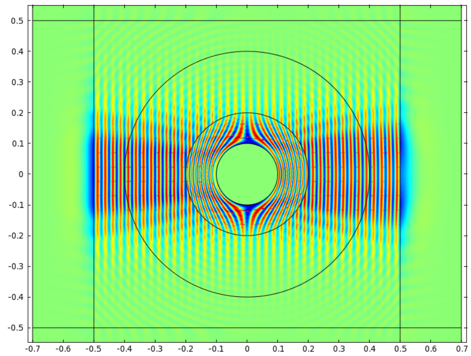

Figure 10: Simplified Simulation Design

The amount of scattering was quantified by taking the magnitude of the difference between the field with the cloak and the field with no object or cloak (a completely undisturbed field).

$$E_{scattered} = |E_{cloak} - E_{no\ object}| \tag{7}$$

Plots were then created comparing both the average scattering and the maximum scattering for various values of ϵ_{min} and μ_{min} between 0 and 1.25. In Figure 11a, the average scattering (top subplot) shows a slightly upward trend as ϵ_{min} increases, although the maximum scattering (bottom suplot) surprisingly decreases. For varied values of μ_{min}, both plots show a roughly increasing value of scattering as μ_{min} increases. Comparing the y-axis ranges for the plots in 11a and 11b, it's apparent that variation in μ_{min} has a greater impact on the simulation than variation in ϵ_{min}, at least for the range of values tested. From this I drew a tentative conclusion that the value for μ_{min} could be the more important value for the performance of the cloak. In order to get a better idea of the scattering, several data sets were selected based on providing a good balance between low maximum scattering and low average scattering. The full data sets for these are plotted in Figure 12. The three data sets plotted show approximately the same pattern of scattering. The amount of scattering is fairly low for most points on the circle, with a peak between 150-200 degrees. In the plot, an angle of 0 degrees corresponds to the point (-0.4, 0) on the circle, while 180 degrees corresponds to (0.4, 0). This corresponds well to the COMSOL simulation plots; the most noticeable scattering is on the right side of the domain, after the wave has passed through the cloak. These results are promising, as it suggests that for the most part the cloak functions well with minimal scattering aside from a relatively small portion of the domain.

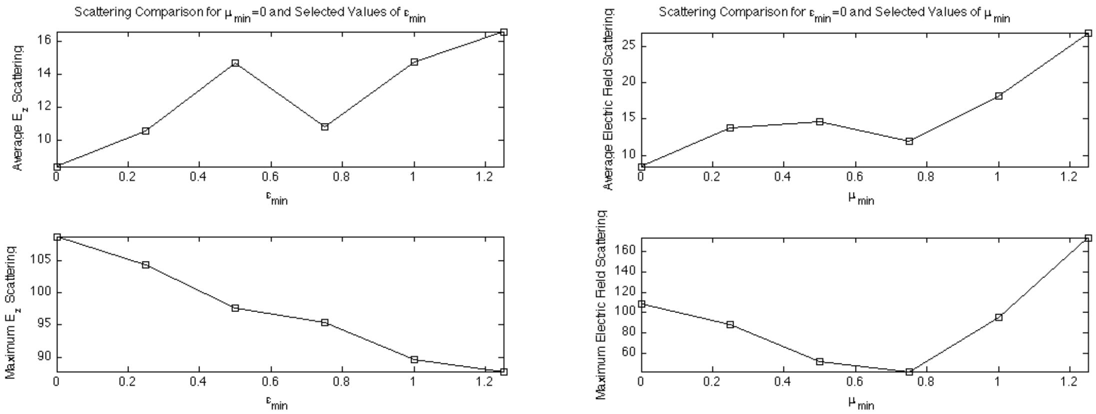

(a) $\mu_{min} = 0, \epsilon_{min}$ varied

(b) $\epsilon_{min} = 0, \mu_{min}$ varied

Figure 11: Scattering Comparisons

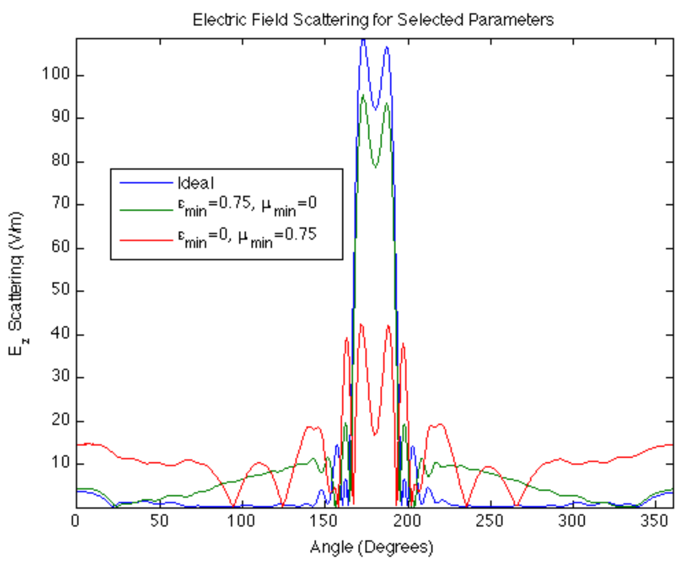

Figure 12: Scattering Comparison for Full Angular Range

Given that it's necessary to maintain the contraints given in Equation 4, the next step was to set $\epsilon_{min} = 1/\mu_{min}$ and vary μ_{min}. Although ϵ has a lower limit of 1, values of μ slightly less than one are physically achievable [7]. The value for ϵ_{min} must be scaled correspondingly, such that their product is always 1. Along with determining the best set of parameters for cloaking a TE wave, the tranverse-magnetic (TM) wave simulation is also addressed. The design of this cloak is very similar to that for a TE wave, except the parameters of interest are now $\epsilon_r, \epsilon_\phi$, and μ_z. Again simplifying the requirements from Equation 1, and then applying our desired constraints, this cloak is decribed in Equation 8.

$$\epsilon_r = max\left(n\left(\frac{r-R_1}{r}\right), \epsilon_{min}\right), \quad \epsilon_\phi = max\left(n\left(\frac{r}{r-R_1}\right), \epsilon_{min}\right),$$

$$\mu_z = max\left(n\left(\frac{R_2}{R_2-R_1}\right)^2, \mu_{min}\right) \tag{8}$$

To create a TM wave, the surface current was oriented in the y-direction, as opposed to the z-direction in the TE case. The only other modification was to change the PMC boundary to a perfect electric conductor (PEC) boundary.

Several values for μ_{min} were tested, for both the TE and TM case, and the results shown in Figure 14. In Figure 14b, the value being plotted is H_z, since this is the out-of-plane component for a TM wave. Given that E_z and H_z have drastically different scales, both figures were scaled by the maximum field value in the no object case. That is, the value plotted is $\frac{E_{scattered}}{E_{max}}$, where E_{max} is the maximum electric field when there is no cloak or scattering object in the domain. For the TM wave the same method is used, in this case plotting $\frac{H_{scattered}}{H_{max}}$. Although this is not a perfect comparison, it provides us with an idea of the magnitude of the scattering relative to the magnitude of the field in the entire domain.

Based on these plots, there appears to be a similar amount of scattering in both the TE and TM case, although the TE case seems to have less scattering overall. In the TE case, the least amount of scattering occurs with $\epsilon_{min} = 1.25$, $\mu_{min} = 0.8$, with average scattering of $0.095E_{max}$ and maximum scattering of $0.296E_{max}$. In the TM case it occurs when $\epsilon_{min} = 1$, $\mu_{min} = 1$, with average scattering of $0.129H_{max}$ and maximum scattering of $0.673H_{max}$. Although this maximum value appears fairly large, the peak scattering occurs between a small range from about 170-190 degrees, with the scattering outside of that range all at $0.315H_{max}$ or less. This suggests that the cloak is still performing well.

The simulations for these parameters are compared to the ideal case in Figures 14 and 15. In Figure 14, we can see that the non-ideal cloak is still fairly close to the ideal case, with the most noticeable distortion on the right half of the domain between about $y = 0.1$ and $y = -0.1$. In the ideal TM case (Figure 15a), manually adjusting the axes made the simulation more difficult to interpret, so it is left with the axes imposed by COMSOL and therefore does not have the same axes as 15b. Because the magnetic field is so small, comparing the fields is difficult, but judging from the power flow lines the results for the non-ideal cloak are still fairly close to those for the ideal cloak. In both the TE and TM case, the cloaks satisfy Equation 3 in the broadband case while still maintaining reasonable performance.

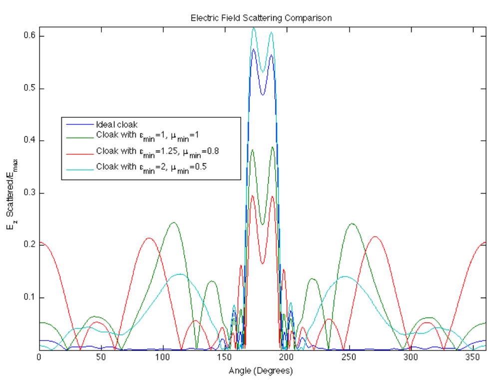

(a) TE Wave

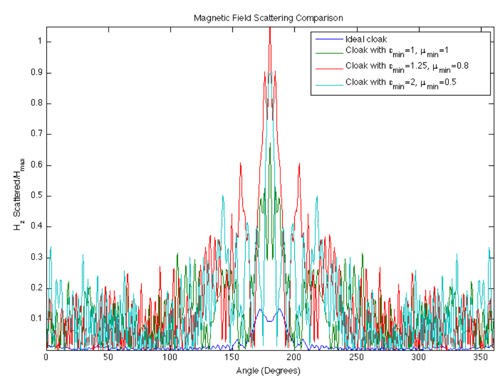

(b) TM Wave

Figure 13: Scattering Comparison for Physically Realizable Parameters

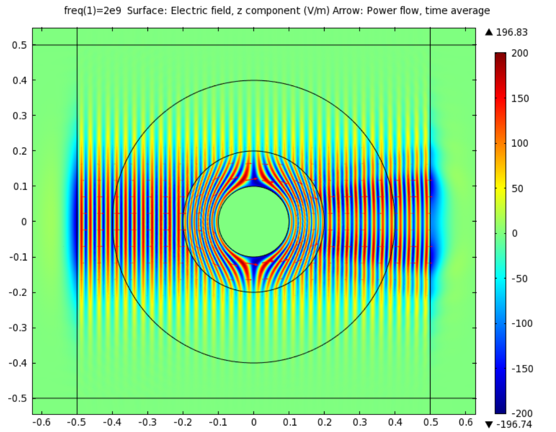

(a) Ideal Cloak

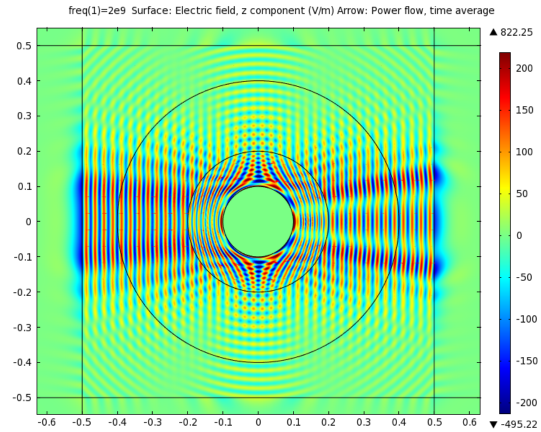

(b) Cloak with $\epsilon_{min} = 1.25, \mu_{min} = 0.8$

Figure 14: Simulation for TE Wave

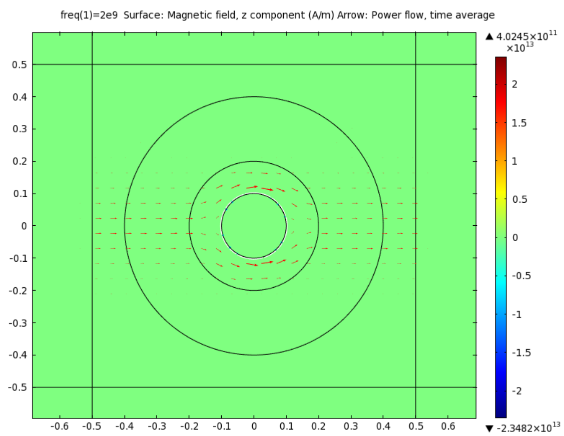

(a) Ideal Cloak

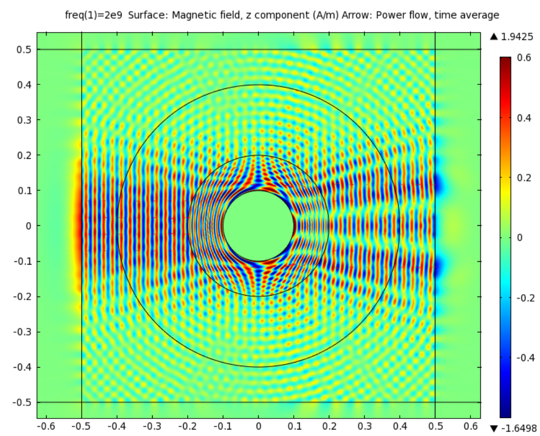

(b) Cloak with $\epsilon_{min} = 1, \mu_{min} = 1$

Figure 15: Simulation for TM Wave

4 Conclusion

An electromagnetic cloak was designed which adheres to the constraints necessary for it to be physically realizable, while still functioning well as a cloak. The cloak was embedded in a background material of $n = 6$ and studied in a 2D domain. In the TE case, the minima which provided the best performance were $\epsilon_{min} = 1.25, \mu_{min} = 0.8$. In the TM case, the best performance was for $\epsilon_{min} = 1, \mu_{min} = 1$. In both cases, although some scattering was evident in the simulations, they were still very close to the ideal case.

The next step in the design of this cloak would be to design a composite material with the desired electromagnetic properties. Cloaking can be physically realized with metamaterials, which are engineered materials designed to bend electromagnetic waves in a manner not normally found in nature. Many of these designs [7, 8] use resonant materials which, due to their frequency-dependence, are not applicable to the design of a broadband cloak. However it is possible to design a broadband cloak when embedding the cloak in a ground-plane background material with refractive index $n > 1$, as studied by Liu et al. [6]. Although ground-plane cloaking is simpler to achieve than cloaking an object in open air, the success of this method suggests that designing the metamaterials for the cloak in this paper should be achievable.

References

[1] J. B. Pendry, D. Schurig, and D. R. Smith, "Controlling electromagnetic fields," *Science*, vol. 312, no. 5781, pp. 1780–1782, 2006.

[2] H. Chen, C. T. Chan, and P. Sheng, "Transformation optics and metamaterials," *Nat Mater*, vol. 9, no. 5, pp. 387–396, 05 2010.

[3] S. A. Cummer, B.-I. Popa, D. Schurig, D. R. Smith, and J. Pendry, "Full-wave simulations of electromagnetic cloaking structures," *Phys. Rev. E*, vol. 74, p. 036621, Sep 2006.

[4] U. S. Inan and A. S. Inan, *Electromagnetic Waves*. Prentice Hall, 2000.

[5] D. J. Griffiths, *Introduction to Electrodynamics*. Prentice Hall, 1998.

[6] R. Liu, C. Ji, J. J. Mock, J. Y. Chin, T. J. Cui, and D. R. Smith, "Broadband ground-plane cloak," *Science*, vol. 323, pp. 366–369, 2009.

[7] B. Wood and J. Pendry, "Metamaterials at zero frequency," *J. Phys.: Condens. Matter*, vol. 19, no. 7, p. 076208, 2007.

[8] D. Schurig, J. J. Mock, B. J. Justice, S. A. Cummer, J. B. Pendry, A. F. Starr, and D. R. Smith, "Metamaterial electromagnetic cloak at microwave frequencies," *Science*, vol. 314, no. 5801, pp. 977–980, 2006.